



# Effects of illegal gold mining on Hg concentrations in water, *Pistia stratiotes*, suspended particulate matter, and bottom sediments of two impacted rivers (Paraíba do Sul River and Muriaé River), Southeastern, Brazil

Philippe Ribeiro Gomes · Inácio Abreu Pestana ·  
Marcelo Gomes de Almeida · Bráulio Cherene Vaz de Oliveira ·  
Carlos Eduardo de Rezende

Received: 4 May 2022 / Accepted: 10 September 2022 / Published online: 17 September 2022  
© The Author(s), under exclusive licence to Springer Nature Switzerland AG 2022

**Abstract** Recent reports of illegal small-scale alluvial gold mining activities (locally called *garimpo*) by miners working on rafts in the Paraíba do Sul River (PSR) and in one of its tributaries (Muriaé River (MR)) have raised concerns about Hg contamination. This study aimed to evaluate the impact of *garimpo* activities on Hg contamination in three environmental compartments. Water, sediment, and aquatic macrophytes (*Pistia stratiotes*) were sampled during the rainy season in PSR, forming a 106-km transect from the point where *garimpo* rafts were seen and/or seized by the Federal Police. They were also sampled in the MR. Total and dissolved mercury (Hg) concentrations in water and total Hg in the suspended particulate matter (SPM) sampled in the PSR increased by 1.7, 1.5, and 2.1 times at the points where the rafts were seen compared to the point immediately upstream. In the MR, Hg concentrations were higher

than those in the PSR, but most values in the environmental compartments were below the safe limits (174–486 ng•g<sup>-1</sup>, threshold and probable effect level, respectively), with the exception of Hg in the SPM of one of the MR sampling points (256 ng•g<sup>-1</sup>) and the mining tailings (197 ng•g<sup>-1</sup>). Sediment granulometry was exponentially associated with Hg concentrations in the sediment ( $R^2=0.75$ ,  $p<0.0001$ ) and is also essential to understand the physical impacts of *garimpo* on PSR. Future studies should focus on assessing the seasonal variability of Hg concentrations in the studied compartments, especially if *garimpo* is identified during the dry season.

**Keywords** Gold mining · Mercury · Sediment · Paraíba do Sul River · Muriaé River

**Supplementary Information** The online version contains supplementary material available at <https://doi.org/10.1007/s10661-022-10477-y>.

P. R. Gomes (✉) · I. A. Pestana · M. G. de Almeida ·  
B. C. V. de Oliveira · C. E. de Rezende  
Programa de Pós-Graduação Em Ecologia E Recursos  
Naturais, Laboratório de Ciências Ambientais,  
Centro de Biociências E Biotecnologia, Universidade  
Estadual Do Norte Fluminense Darcy Ribeiro,  
Av. Alberto Lamego, 2000 – Parque Califórnia,  
Campos dos Goytacazes, Rio de Janeiro CEP: 28013-602,  
Brazil  
e-mail: philipe0805@gmail.com

## Introduction

Environmental contamination by metals poses a serious threat to the environment and to food security due to the accelerated development of agriculture and industry, as well as the disturbance of natural ecosystems due to the high increases in the worldwide population (Sarwar et al., 2017). High concentrations of metals in soils, sediments, and water resulting from anthropogenic activities can lead to harmful biota and human health effects (Franz et al., 2013; Gamvroula et al., 2013; Alexakis, 2020; Dall’Agnol et al., 2022). Indeed, arsenic, lead, mercury, and cadmium are

ranked among the top ten pollutants in the priority list ranking of the American Agency for the Toxic Substances and Diseases Registry (ATSDR, 2019), a list that employs compound toxicity and human exposures as criteria for ranking the frequency in which toxic substances are found in facilities containing hazardous waste. Among these elements, mercury (Hg) has been classified for 30 years as the third leading pollutant in this ranking.

Environmental contamination by Hg is associated with several anthropogenic activities, such as fossil fuel burning, industrial activities, solid waste disposal, and forest clearing (Selin, 2009; Dall'Agnol et al., 2022). Among these activities, small-scale alluvial gold mining (locally called *garimpo*) is noteworthy, known as the most significant Hg pollution source worldwide (Esdaile & Chalker, 2018). Because of this, the reform of this activity is considered a priority in the Minamata Convention on Hg that aims to reduce and eliminate Hg use and the production of Hg-containing products (UNEP, 2013). Brazil acceded to the treaty in 2018 (Brasil, 2018). The main actions taken by the countries participating in this treaty include banning the opening of new mines for Hg extraction, regulating the use of Hg in *garimpo* activities and in the production of everyday items, such as fluorescent lamps and batteries (UNEP, 2017).

*Garimpo* activities carried out by rafts dredge the bottom sediments from rivers and employ metallic Hg ( $\text{Hg}^0$ ) to form a gold-Hg amalgam that is later burned using a gas torch in the open to volatilize the Hg and recover the gold (Guimaraes, 2020; Pestana et al., 2022). Estimates indicate that for each 1 kg of gold produced through *garimpo* activities, 1.3 to 1.7 kg of Hg are released into the environment (Hacon et al., 1990; Pestana et al., 2022; Pfeiffer & Lacerda, 1988), with emissions from this activity higher in South America compared to all other regions of the globe (UNEP, 2019). It is estimated that of all the Hg employed in this activity, 54% are released into the atmosphere in the form of vapor and 46% are released into rivers as  $\text{Hg}^0$  (Hacon et al., 1990; Pfeiffer & Lacerda, 1988), which can become methylated and bioaccumulate in exposed biota (Lacerda & Malm, 2008). Epidemiological studies indicate that the Amazon region is one of the most Hg-exposed areas worldwide (Passos & Mergler, 2008), and studies in southeastern Brazil

have already reported contamination of sugarcane workers exposed to organomercurial pesticides in the past (Câmara, 1986, 1990, 2017). In addition to environmental Hg contamination, gold miner exposure to Hg vapors during gold-Hg amalgam burning causes severe damage to the central nervous system, as these vapors accumulate in the brain (Lauthartte et al., 2018; Li et al., 2015).

In the scientific literature, gold mining in the Paraíba do Sul River (PSR), located in southeastern Brazil, and consequent Hg contamination of surrounding aquatic ecosystems have been reported as a past event until now. Indeed, the PSR has a history of Hg contamination due to two anthropogenic activities that took place in the 1970s and 80 s: i.e., widespread *garimpo* activities and the use of organomercury fungicides in sugarcane plantations, as stated previously (Almeida & Souza, 2008; Lacerda et al., 1993). Chronologically, this *garimpo* activity began in the Muriaé River (MR), a tributary of the PSR, and later extended to the Itabapoana River (Lima, 1990). In 1980, the use of Hg agrochemicals was banned due to the intoxication of sugarcane workers by Hg (Brasil, 1980; Câmara, 1986, 1990). Seven years later, *garimpo* activities were prohibited in the PSR and its tributaries, in view of the risk of Hg contamination (Almeida & Souza, 2008). Indeed, Hg atmospheric deposition has decreased from the late 1970s to the present ( $15\text{--}30 \mu\text{g}\cdot\text{m}^2\cdot\text{year}^{-1}$ ) as a result of emission control measures implemented at that time (Lacerda & Ribeiro, 2004).

The events listed above and the prohibitions that resulted from them limited the activities of the gold miners in the PSR in the ensuing years. However, the context of the COVID-19 pandemic, associated with economic and political factors, motivated a new wave of *garimpo* in the PSR and MR at the end of 2021 (Folha): (a) the price of gold increased by 90% compared to pre-pandemic values, reaching R\$ 320 per gram (Pontes, 2021), making the activity even more attractive; (b) the reduction in the number of people for environmental control in Brazil, favoring the advancement of illegal *garimpo* activities throughout the country, such as the recent invasion of the Madeira River (Amazonas) by hundreds of rafts and dredges (Pestana et al., 2022; Prazeres, 2021; Thomas, 2021); and (c) the federal government's pro-*garimpo* agenda, especially in the Amazon region, which has implicitly encouraged miners across the country to return to the

activity (Guimaraes, 2020; Pestana et al., 2022). For example, the government issued two decrees (Brasil, 2022a; Brasil, 2022b) that encourage *garimpo* in the Amazon and proposed the development of the state through this activity. This is in the opposite direction of preservation, not only in the Amazon, but elsewhere in the country, since *garimpo* is unsustainable by definition (Guimaraes, 2020).

In October 2021, the Environmental and Military Police identified an illegal mining raft located in the PSR near the city of Itaocara, in the state of Rio de Janeiro (Trindade, 2021). One month later, the Federal Police launched “Operação Paraíba Dourado” (which means “Golden Paraíba,” in a literal translation) and four rafts were seized between the city of Cambuçi and Pureza, a district of the city of São Fidélis (Folha de Itálva, 2021a; Trindade, 2021). In the MR, there were also reports of an increase in *garimpo* activities since July 2021 (Folha de Itálva, 2021b; Jornal Terceira Via, 2021). Previous studies conducted in this drainage basin indicated high Hg concentrations in several fish species, especially demersal ones (up to  $0.3 \mu\text{g}\cdot\text{g}^{-1}$ ), indicating the significant role of *garimpo* activities concerning Hg biota exposure (Azevedo et al., 2017, 2018; Rocha et al., 2015).

In this context, this study aimed to evaluate the impact of *garimpo* activities on Hg contamination in three environmental compartments (sediment, water, and aquatic macrophytes) along a 106-km transect, starting from the point where the mining rafts were seized. Monitoring the impact of small-scale alluvial mining gold mining on Hg contamination is paramount, as *garimpo* remains the main source of Hg contamination for aquatic ecosystems in Latin America (Meneses et al., 2022). Higher Hg concentrations near the points where *garimpo* rafts were seized and/or seen are expected, as (I) the  $\text{Hg}^0$  used in the amalgamation of gold is insoluble in water, and (II) the effects of *garimpo* are spatially limited (Lechler et al., 2000; Guimaraes, 2020).

## Material and methods

The PSR is formed by the union of the Paraíba and Paraitinga rivers, whose sources are located in the state of São Paulo. It travels a distance of approximately 1100 km to its mouth, located at Atafona

Beach (municipality of São João da Barra), where it flows into the Atlantic Ocean (Fig. 1). Its watershed is located in the most populous and industrialized area of the country (Southeast Brazil), with a total drainage area of  $61,307 \text{ km}^2$ , divided among the states of Rio de Janeiro ( $26,674 \text{ km}^2$ ), São Paulo ( $13,934 \text{ km}^2$ ), and Minas Gerais ( $20,699 \text{ km}^2$ ). In addition, its upper and middle watersheds are constituted by rocks formed during the Precambrian period, predominantly migmatites, biotite, biotite-gneiss schists, granitoid gneisses, and quartzite invasions. The lower coastal plain basin is formed by tertiary and quaternary lands (DNPM, 1983). It is a river under federal control and its main tributaries are the rivers Pomba, Muriaé, and Paraíba Mineiro (on the left bank), and Piabanha, Piraí, and Dois Rios (on the right bank) (AGEVAP, 2018). The highest flows are observed in the rainy season (December to February), with an average of  $4624 \text{ m}^3\cdot\text{s}^{-1}$ , and the lowest in the dry season (June to August), with an average of  $115 \text{ m}^3\cdot\text{s}^{-1}$  (Almeida & Souza, 2008).

Campos dos Goytacazes is the largest city in the state of Rio de Janeiro and the penultimate city that the PSR passes through before flowing into the ocean. Its estimated population is of over 500,000 people (IBGE, 2021). Solid waste produced by the population of Campos dos Goytacazes and five other neighboring cities is collected and taken to a sanitary landfill in the district of Conselheiro Josino, which receives approximately  $450 \text{ tons}\cdot\text{day}^{-1}$  (Almeida et al., 2019). Although solid waste is a potential source of Hg contamination, mainly due to the disposal of fluorescent lamps and batteries (Cheng & Hu, 2012), this contribution is not relevant to the study areas, as the landfill is located more than 35 km away from the PSR.

Watershed Hg sources may include the runoff of legacy Hg in soils from past activities, including the use of organomercurials in sugarcane plantations and *garimpo* activities (Câmara, 1986; Lacerda et al., 1993), in addition to industrial discharges in the upper part of the river, in the city of Rio de Janeiro (Veck et al., 2007). Although two small hydroelectric plants are located at the lower part of the PSR (namely Santa Cecília and Ilha dos Pombos), which could limit Hg suspended particulate matter (SPM) transport downstream, they are located at 184 and 357 km from the study area and, therefore, their impacts on Hg dynamics should not be locally significant (AGEVAP,

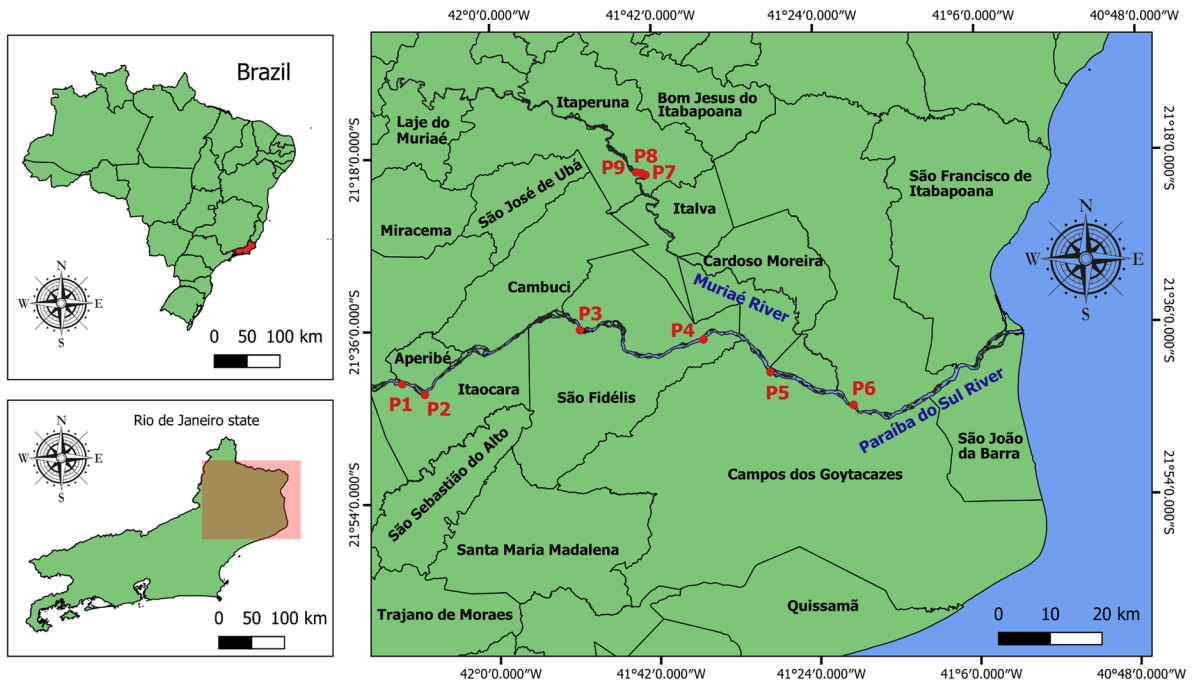


**Fig. 1** Map of Brazil and the state of Rio de Janeiro (red) showing the sampling points (P1 to P6) in the Paraíba do Sul River (ca. 106 km transect) and Muriaé River

2018). Furthermore, as  $Hg^0$  is insoluble, a significant influence from sources distant from the study area on the data interpretation is not expected.

The MR is one of PSR tributaries and is located in the lower portion of the basin (Fig. 1). It has a length of 300 km and a total drainage area of 8162 km<sup>2</sup>. It is formed by the union of the Bom Sucesso and Samambaia rivers. It flows in a flat region, forming a floodplain in periods of large floods from the municipality of Italva to its mouth. It covers 26 municipalities, the most representative in terms of population being Muriaé, Itaperuna, and Carangola (ANA, 2022). Approximate channel width and depth for the PSR and MR are 494 and 96 m, and 7 and 2 m, respectively.

In the PSR, six sampling points were defined, forming a transect of 106 km between them. The sampling was carried out in December 2021 and P2 and P4 are the sampling points where illegal mining rafts were seized and/or seen, in the districts of Batatal and Pureza, respectively (Folha de Italva, 2021a; Trindade, 2021). At the MR, three points were sampled in January 2022, when illegal mining rafts were sighted (Fig. 2a, b). Points P8 and P7 are located upstream and downstream of the *garimpo* area,

respectively. Local MR residents denounced the presence of illegal mining rafts that had been operating in the region since June 2021 (Folha de Italva, 2021b; Jornal Terceira Via, 2021). At the sampling points, the engine of one of the rafts' dredges was observed in active operation (Fig. 2b). In addition, *garimpo* tailings were observed on the banks of the river (Site P9; photo image in Fig. 2c), which were also sampled concerning Hg concentrations. As stated previously, the samplings were carried out in view of denunciations and reported raft sightings. In this sense, seasonality, river discharges, and land use effects on Hg dynamics could not be included in the sample design.

Water and surface sediment samples were collected at all sampling points (P1 to P8) during the morning (09 AM–12 PM). Surface water ( $\pm 10$  cm) and surface sediment were sampled in the main channel of each river ( $n=5$  independent samples for both matrices at each sampling point). Water samples were stored in pre-rinsed bottles with water from the same sampled point and sediment samples were stored in plastic bags. Aquatic macrophytes were only present at P1 and P2, where *Pistia stratiotes* specimens were sampled. The macrophytes were separated into roots

**Fig. 2** Illegal *garimpo* activity in the Muriaé River. **a** Illegal raft with engine turned off at the time of photography. We were able to approach this raft because there were no gold miners working (*garimpeiros*) on it at the time of the photograph. **b** Illegal raft with engine running at the time of photography. Due to the risk of a possible retaliation, this photograph was taken from afar because there were *garimpeiros* working on this raft. **c** Tailings from *garimpo* activity on the banks of the Muriaé River. More tailings were also found along the river channel



and shoots and stored in plastic bags. At P9, only tailings from *garimpo* activities located on the banks (less than 1 m away from the river) of the MR were sampled. All samples were packed in thermal boxes and transported to the laboratory for processing.

The physicochemical parameters of the water column, such as pH, temperature (DM-2P, Digimed, Brazil), electrical conductivity (DM-3P, Digimed, Brazil), and dissolved oxygen (Model 55-12FT, YSI, USA) were measured in situ at all sampling points, with the exception of P9 (S1). The electrodes were periodically calibrated with buffer solutions to avoid measurement errors and the precision was of  $\pm 0.01$  for all physicochemical parameters.

At the laboratory, the water samples were filtered using GF/F Whatman® filters (0.7- $\mu\text{m}$  porosity) (Pestana et al., 2019). During the entire procedure, gloves were used to avoid Hg contamination. Likewise, all glassware was previously washed with nitric acid ( $\text{HNO}_3$ ) and hydrochloric acid (HCl, 24-h baths for each acid) and subsequently rinsed with ultrapure water three times. Hg determinations were performed on the same day of sample filtering, in order to prevent Hg losses (Kasper et al., 2015). The filters were dried and weighed beforehand on an analytical balance (Model ME-5, Sartorius, Germany), and after filtration they were once again dried in an oven ( $< 40\text{ }^\circ\text{C}$ ) and then weighed to obtain the mass of SPM.

Total Hg concentrations were determined in both unfiltered (total Hg in water) and filtered water samples (dissolved Hg in water < 0.7 µm). The Hg concentrations in the SPM were obtained by subtracting the dissolved Hg concentrations from the total Hg concentrations, and the result was divided by the SPM concentrations.

For the analysis of total and dissolved Hg, 300 µL and 150 µL of 0.2 N bromine chloride (BrCl) were added in 30-mL aliquots of the unfiltered and filtered water samples, respectively. Prior to the determination, 150 µL of BrCl, 60 µL of hydroxylamine hydrochloride (NH<sub>2</sub>OH·HCl), and 150 µL of stannous chloride (SnCl<sub>2</sub>) were added to the samples. Analytical blanks were included ( $n=3$ ) in all analyses. The determination of total and dissolved Hg was performed by atomic fluorescence spectrophotometry using the cold vapor generation technique (CV-AFS Mercury Analysis System, Model 2600, Tekran Instruments Corporation, Toronto, Canada) calibrated with a 7-point curve (0.33, 0.83, 1.66, 3.33, 8.32, 16.35, and 33.33 ng·L<sup>-1</sup>). The method detection and quantification limits were 0.06 and 0.2 ng·L<sup>-1</sup>, respectively. A certified estuarine sediment sample (NIST 1646A) was used to evaluate the accuracy of the method and the obtained Hg recovery was 96.22 ± 0.02% ( $n=5$ ). Reproducibility was assessed using analytical triplicates every 20 samples (coefficient of variation < 15%).

The surface sediments were lyophilized (Freeze-Dry System, Labconco, Model 7,522,900, Kansas City, USA) and then separated into the fraction of interest (sieve < 2 mm) for Hg determination and for granulometric analysis. For Hg determination, the samples were macerated with the aid of a mortar and pestle and then packed in polyethylene bags and stored until analysis.

The aquatic macrophyte (*Pistia stratiotes*) samples were lyophilized, separated into roots and leaves, and ground in a knife mill (Model MA048, Moinho Marconi, SP, Brazil) for homogenization. The samples were packed in polyethylene bags and stored until analysis.

Dry aliquots of 0.3 g of sediment were solubilized in 8 mL of aqua regia (3 HCl: 1 HNO<sub>3</sub>), and 0.3 g aliquots of macrophyte tissues (leaf and root) were solubilized with 4 mL of ultrapure water + 2 mL of hydrogen peroxide (H<sub>2</sub>O<sub>2</sub>) + 6 mL of H<sub>2</sub>SO<sub>4</sub>:HNO<sub>3</sub> (1:1) (according to the protocol described by Silva-Filho

et al. (2006)). The extracts were solubilized in a microwave oven (Mars Xpress, CEM, Model 907,501, USA). The total digestion time for the sediment and macrophyte tissues was 35 min (10 min, until reaching 95 °C; and 25 min with constant temperature of 95 °C) with power of 1600 W (adapted from Bastos et al., 1998).

After cooling for 30 min, the extracts (sediment and macrophyte tissues) were filtered through Whatman® 40 paper and placed in tubes, which were filled to 25 mL with ultrapure water (Milipore Milli-Q, Integral model A10, Molsheim, France). After that, 1 mL of each final extract was added to 29 mL of ultrapure water and then 150 µL of BrCl, 60 µL of NH<sub>2</sub>OH·HCl, and 150 µL of SnCl<sub>2</sub> were added. In all analyses, analytical blanks were included ( $n=3$ ). The Hg determination in the sediment and tissues of the macrophytes was also performed by atomic fluorescence spectrophotometry using the cold vapor generation technique.

The granulometric analysis of the sediment samples was performed using a laser diffraction particle analyzer (Model SALD-3101, Shimadzu, Japan). Each sample was subjected to ultrasonic agitation for 10 min to disaggregate the particles before determining the particle size distribution (Blott et al., 2004; McCave et al., 1986). Fractions were classified according to Krumbein and Aberdeen (1937).

To evaluate Hg dynamics in the water column, a geochemical partition coefficient (K<sub>d</sub>-Hg) between the particulate and dissolved fraction was determined by the following formula:

$$K_d - \text{Hg} (\text{L} \cdot \text{g}^{-1}) = \frac{\text{Log} (\text{Hg in SPM} (\text{ng} \cdot \text{g}^{-1}))}{\text{dissolved Hg} (\text{ng} \cdot \text{L}^{-1})} \quad (1)$$

Statistical analyses were performed using the R statistical program (R Core Team, 2021). Empirical combinatorial analyses (Monte Carlo Method; Khitalishvili, 2016) were used to calculate the ratios of Hg concentrations between the sampled environmental compartments, including the K<sub>d</sub>-Hg, in order to incorporate the variability of Hg concentration in each compartment in the final result.

An analysis of variance (ANOVA) was used to evaluate the effect of the distance from the PSR mouth on total, dissolved, particulate, and sediment Hg concentrations. When an effect was detected,

multiple comparisons among the sampling points were performed using the Tukey test and significant differences were reported using the compact letter display (Mendiburu, 2021).

Regressions between total Hg concentrations and the silt+clay content of the sediments were used to assess the association between these two variables. The model equation, determination coefficient ( $R^2$ ), and  $p$ -values were computed. A maximum likelihood function (Venables & Ripley, 2002) was used to perform transformations of the data, when necessary, in order to meet the premises of ANOVA and regressions (normality, linearity, homoscedasticity of residuals). ANOVA and regression results were validated using diagnostic plots (Altman & Krzywinski, 2016). In all cases, an a priori type I error of 5% ( $\alpha=0.05$ ) was assumed.

### Results and discussion

The behavior of Hg concentrations along the transect of the PSR indicated the limited effect of *garimpo* activities on Hg dynamics in aquatic ecosystems,

with the detected patterns independent of water column physicochemical parameters (pH, electrical conductivity, dissolved oxygen and temperature; S2) and SPM loads (S3). The total, dissolved, and particulate Hg concentrations (Fig. 3) were higher at the points where the rafts were seen and/or seized compared to the immediately previous (upstream) point of the transect by factors of  $1.7 \pm 0.7$ ,  $1.5 \pm 0.2$ , and  $2.1 \pm 0.8$  times, respectively (Fig. 3). At these same points, where the rafts were located, the highest Hg concentrations were observed for each of these environmental compartments. The behavior of dissolved Hg concentrations along the transect is even more noteworthy: there was a continuous increase in Hg concentrations from the point where the first raft was observed to the point where the second raft was observed, followed by a sharp decrease after the latter.

The pattern of a local increase in Hg concentrations in the water column at the site of *garimpo* activity followed by a rapid decrease has previously been observed by other authors (Diringer et al., 2015; Limbong et al., 2003). This spatial limitation of *garimpo* effects was discussed by Lechler et al. (2000), who analyzed Hg in the

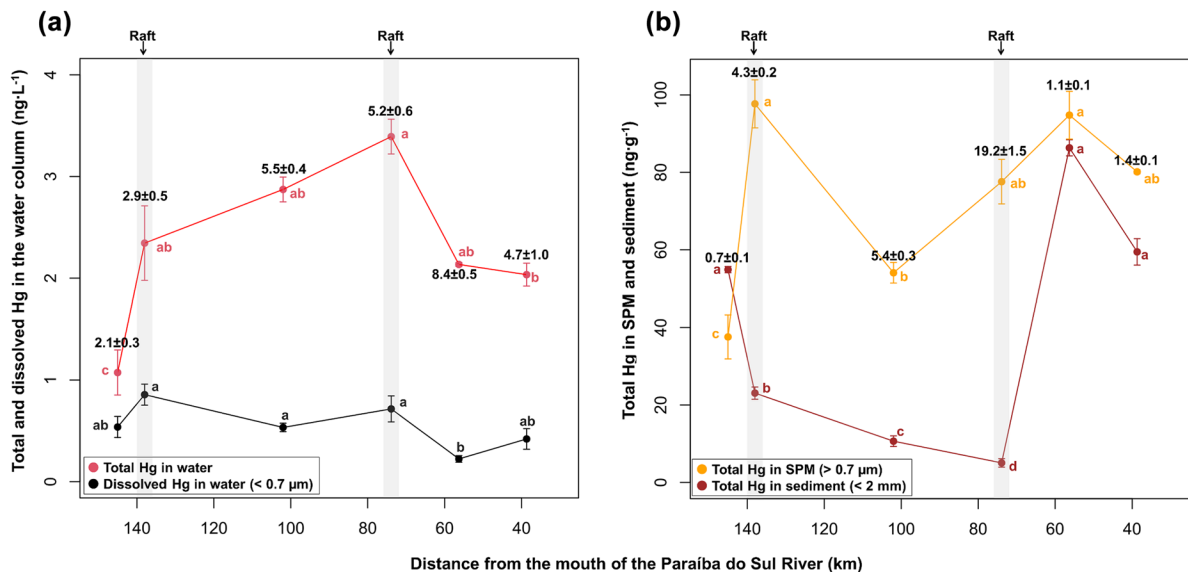


**Fig. 3** Total, particulate, and dissolved Hg concentrations in the Paraíba do Sul River water column, SPM, and bottom sediments. **a** Total and dissolved Hg (< 0.7 μm) in water; **b** total Hg in SPM and bottom sediments. Lowercase letter denotes significantly different mean Hg concentration among the sampling points. The numbers are the mean ± SD of the ratio

between total and dissolved Hg in water and between total Hg in SPM and bottom sediments for each of the sampling points. The points where the rafts were seen and/or seized are highlighted in gray. Each point represents 5 independent samples ( $n=5$ )

water column in a 900-km transect of the Madeira River (corresponding to 62.07% of its length), where *garimpo* activities were and still are intense (Pestana et al., 2022). Comparatively, this study evaluated a transect of only 106 km (corresponding to only 9.38% of the PSR extension). The findings indicate spatial variations in Hg concentrations (coefficients of variation of 74% and 84% for total and dissolved Hg, respectively), but lower when compared to those of Lechler et al. (2000) (coefficients of variation of 85% and 108% for total and dissolved Hg, respectively), suggesting that *garimpo* effects on the PSR are less pronounced than on the Madeira River. This is in line with Guimaraes (2020), who considered that the “limited spatial effects of *garimpo*” apply to specific geographic and social contexts. For example, Lechler et al. (2000) carried out sampling in the Amazon Basin, where Hg concentrations are among the highest in the world, and remarked that the region’s soils play a major role in the Hg cycle, acting as the largest natural reservoir. For southeastern Brazil, on the other hand, the main sources of Hg are from *garimpo* and the use of Hg agrochemicals (Almeida & Souza, 2008; Câmara, 1986, 1990; Lacerda et al., 1993), so this should be taken into account in this type of comparison. In addition, on the Madeira River, hundreds of rafts have been reported (350 rafts; Branches, 2021) when there is *garimpo* activity, while in the PSR the number of rafts was much smaller (four rafts; Folha de Itálva, 2021a; Trindade, 2021).

Total Hg concentrations in the PSR’s sediments exhibit different behaviors from those observed for the mentioned environmental compartments. In this compartment, concentrations were lower at the points where the rafts were seen (Fig. 3b). This result was opposite to what was expected, as gold miners use Hg<sup>0</sup> to amalgamate gold, which has low solubility and accumulates in sediments (Lacerda & Malm, 2008). In this case, the granulometric analysis of the sediment helps to understand this result.

The granulometry data showed that in most sampling points, there was a large percentage of silt + clay content (Fig. 4c), with the exception of precisely the point where one of the rafts was observed (P4, Fig. 4c). The relationship between the silt + clay content and Hg concentrations in the PSR sediment was direct and exponential (Fig. 4b), showing a clear effect of granulometry on Hg concentrations. Normalizing the Hg concentrations in the sediments by the silt + clay content (Fig. 5a), the results indicate that,

proportionally to the amount of silt + clay, P4 presented the highest Hg concentrations in the sediment.

This demonstrates a *garimpo* effect also on Hg concentrations in sediments. The modification of sediment granulometry in *garimpo* areas has been described by other authors (Guimaraes, 2020; Serapião & Ladeira, 2022). According to Guimaraes (2020), *garimpo* areas have a major impact in the silting of rivers, which not only increases the sand content in the sediment but also impacts the diversity and abundance of fish on a spatial scale wider than that described for the impacts of Hg contamination (Mol & Ouboter, 2004).

All Kd–Hg values were greater than 1 (Fig. 5b), demonstrating the high Hg affinity with SPM, which is in line with expectations for the region (Almeida & Souza, 2008). It is also possible to infer that Hg transport occurred preferentially associated with SPM. The Kd–Hg values were within the range (3.1 to 5.9) described by Picado and Bengtsson (2012), who evaluated the Artiguas River (Nicaragua), where *garimpo* activities also occur.

In general, total (2 to 3 ng•L<sup>-1</sup>) and dissolved Hg (0.2 to 0.9 ng•L<sup>-1</sup>) concentrations in water were lower than the limits described by Brazilian regulations (2000 ng•L<sup>-1</sup>–class III freshwater) (CONAMA, 2005). Furthermore, Hg concentrations in the SPM (38 to 95 ng•g<sup>-1</sup>) and sediments (5 to 86 ng•g<sup>-1</sup>) were below the levels at which a small probability of adverse effects on the biota is expected (threshold effect level (TEL) 174 ng•g<sup>-1</sup> and probable effect level (PEL) 486 ng•g<sup>-1</sup>), and lower than the TEL (CCME, 2002), demonstrating little or no risk to the biota. On the other hand, the high values found in sediments (86 ng•g<sup>-1</sup>) were over twofold Hg background levels in PSR basin sediments (40 ng•g<sup>-1</sup>; Souza, 1994).

Hg concentrations were higher in the roots compared to the leaves of the sampled aquatic macrophytes (Table 1). The calculated translocation factors (leaf to root ratio) were less than 1, demonstrating low translocation of Hg to the aerial parts. This was expected, since the roots of these macrophytes are in direct contact with the water column and have a high surface area to adsorb Hg-rich particles (Molisani et al., 2006). The higher Hg accumulation in the roots of macrophytes is a protective strategy, since the restriction of Hg transport to the aerial parts prevents possible damage to the photosynthetic apparatus (Lominchar et al., 2019). This not only indicates that



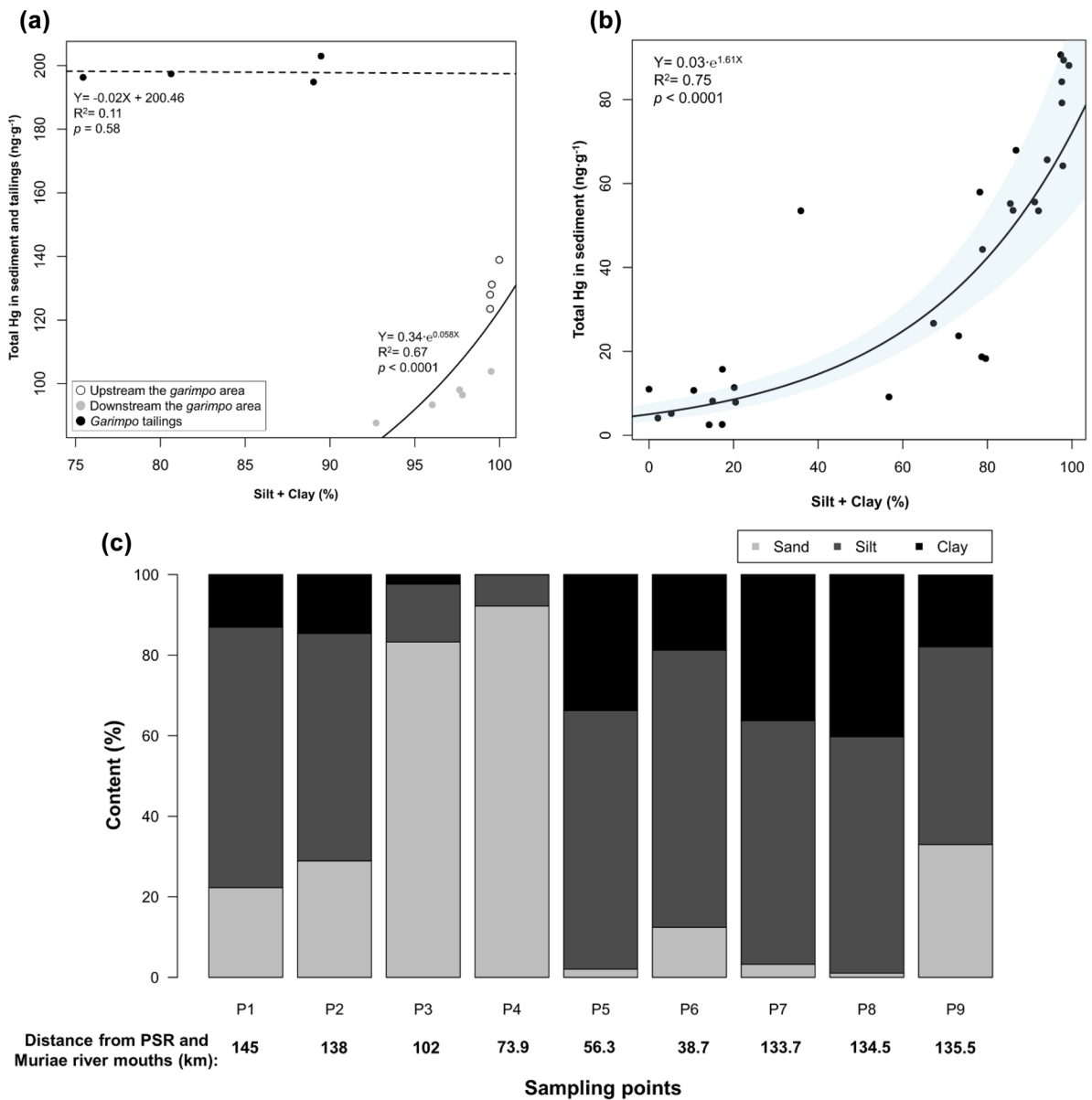


**Fig. 4** a Association of Hg concentrations with silt+clay content of Garimpo tailings (P9) and sediments from the Muriaé River (P7 to P9). The dashed and solid lines represent the regression models associated with the tailings and sediments samples respectively. b Association of Hg concentrations with the silt+clay content of sediments from the Paraiba do Sul

River (P1 to P6). The blue shading indicates the 95% regression model confidence interval and the regression statistics. c Granulometry of sediment samples for each sampling point from Paraíba do Sul River (rafts were seen/seized at P2 and P4) and the Muriaé River (rafts seen at P9)

Hg is mostly accumulated in the roots, but also that it can enter the food chain through ingestion, especially by herbivorous fish (Súarez et al., 2001). It is important to highlight that the macrophytes sampled at the

point where the raft was seen (P2) showed higher Hg concentration in all tissues in comparison with those at P1, which further indicates that the *garimpo* activity also affects the aquatic plant biota.

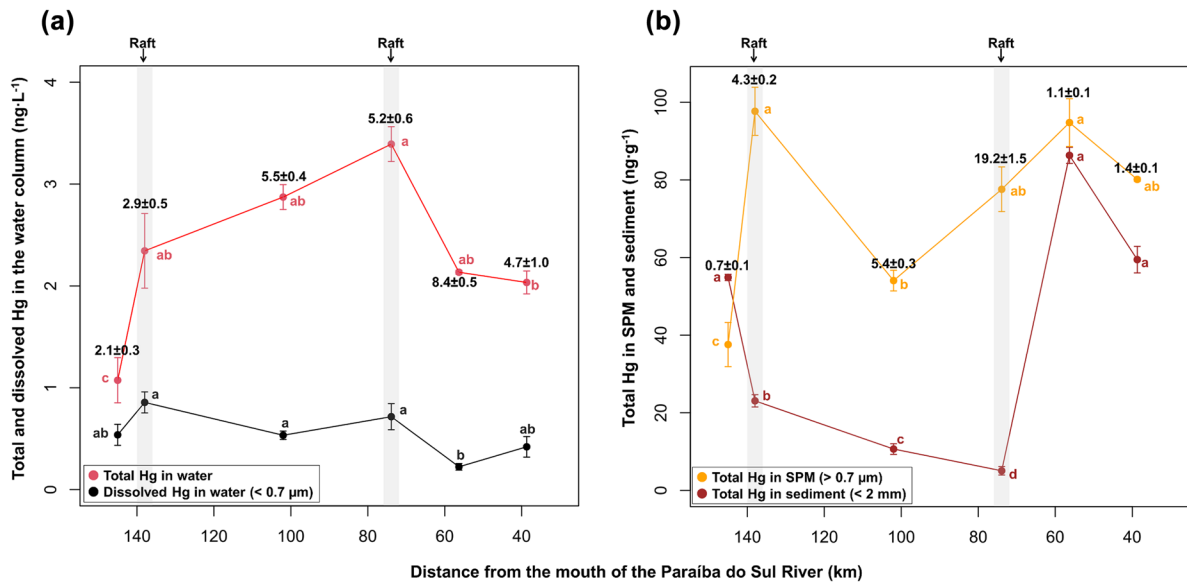


**Fig. 5** **a** Total Hg concentrations in the sediments of the Paraíba do Sul River on the original scale (wine) and the log of Hg concentrations in the sediments normalized by the silt + clay content (blue). **b** Total Hg in SPM and dissolved Hg concentrations in water. The numbers are mean  $\pm$  SD of the Hg geochemical partition coefficient ( $K_d$ -Hg) between these water

column fractions. In both graphs, the lowercase letters indicate significantly different mean Hg concentrations of each environmental compartment among the sampling points. The sampling points where the rafts were seen and/or seized are highlighted in gray. Each point represents 5 independent samples ( $n = 5$ )

In the MR, the mean ( $\pm$ SD) total Hg concentrations in water ( $10 \pm 0.4$  ng·L<sup>-1</sup>), SPM ( $256 \pm 11$  ng·g<sup>-1</sup>), and bottom sediments ( $131 \pm 11$  ng·g<sup>-1</sup>) were higher at the sampling point upstream of the *garimpo* area ( $p = 0.002$ ,  $0.003$ ,  $0.004$ , respectively), while the inverse pattern was observed for dissolved Hg ( $5 \pm 1$  ng·L<sup>-1</sup>;  $p = 0.052$ ) (Fig. 6). In the sediments of these points (P7 and P8), there was predominance of silt + clay content (Fig. 4c), which has a direct and exponential relationship with Hg concentrations ( $R^2 = 0.67$ ,  $p < 0.0001$ ; Fig. 4a).

**Table 1** Total Hg concentration in the tissues of the aquatic macrophyte *Pistia stratiotes* sampled in the Paraíba do Sul River at the points where it was present. Values are mean  $\pm$  SD. Sample size is in parenthesis

Variable	P1	P2
Hg concentration in leaves (ng·g <sup>-1</sup> )	5 $\pm$ 2 (5)	23 $\pm$ 8 (5)
Hg concentration in the roots (ng·g <sup>-1</sup> )	28 $\pm$ 19 (5)	55 $\pm$ 23 (5)
Translocation factor (root/leaf)	0.2	0.4
Distance of the sampling point from PSR mouth (km)	145	138

This may explain the higher Hg concentrations upstream from the *garimpo* area, since at that point the silt + clay content corresponded to  $\approx 100\%$ , while at the point downstream from the *garimpo* area, this value was slightly lower (Fig. 4a). Higher silt + clay contents were expected to be associated with higher Hg<sup>0</sup> accumulations, since this granulometric fraction is an important support for Hg adsorption and immobilization (Moreno-Brush et al., 2020). Besides the granulometry effect, another factor must be considered to explain the higher Hg concentration detected upstream the *garimpo* area: the rafts do not stand still for a long time. Instead, they travel along the river channel. It is possible that the higher Hg concentrations observed upstream from the *garimpo* area is due to remnants of previous activities further upstream, where the flow may have resuspended contaminated sediments that then transported the Hg downstream.

Comparatively, Hg concentrations in the SPM were higher than those in the sediments at both MR sampling points (Fig. 6). This can be explained by the  $K_d$ -Hg values upstream ( $3.95 \pm 0.20$  L·g<sup>-1</sup>) and downstream ( $2.90 \pm 0.37$  L·g<sup>-1</sup>) the *garimpo* area, demonstrating higher Hg affinity with SPM

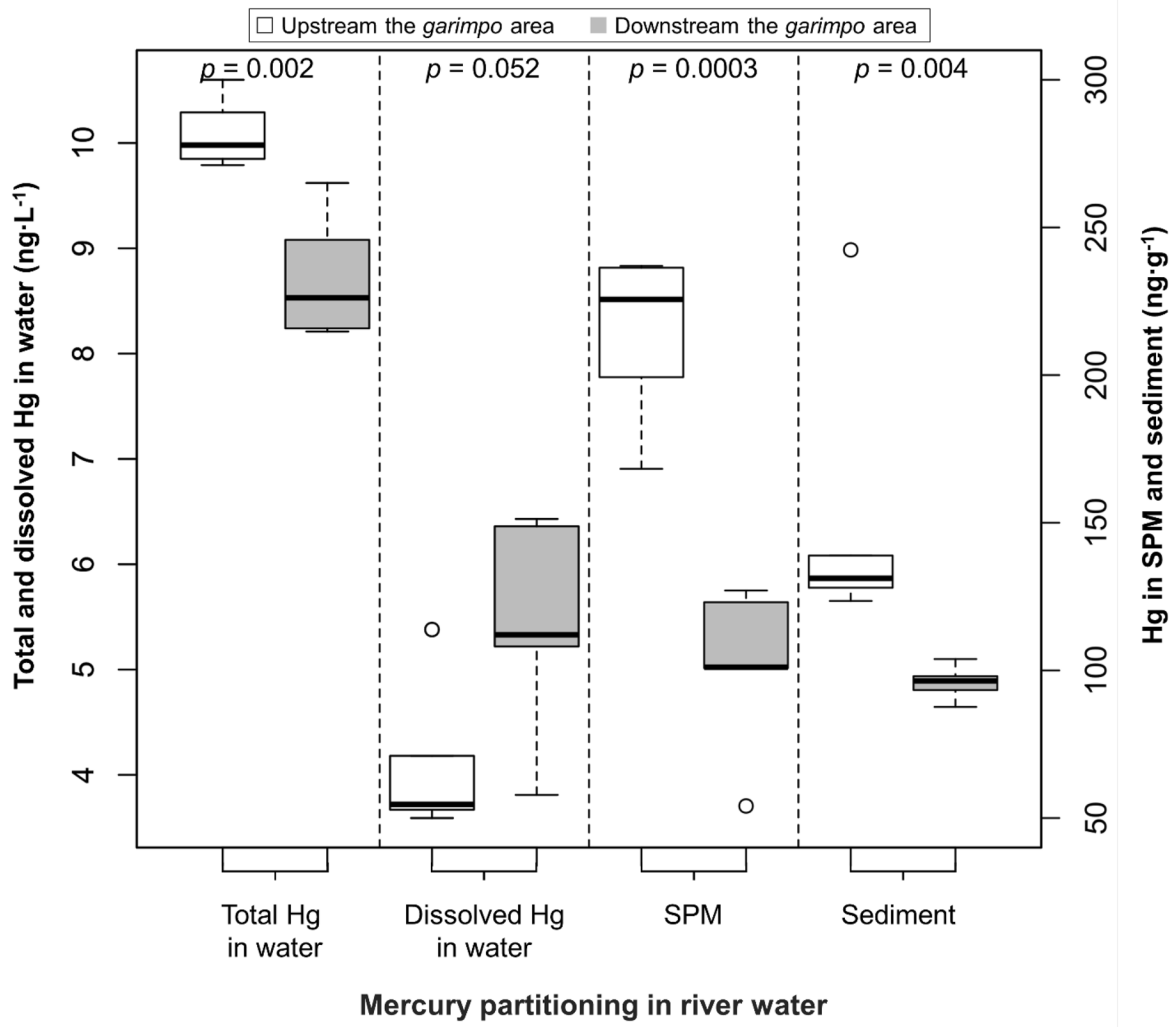


**Fig. 6** Total Hg in sediments, SPM and dissolved concentrations from the Muriaé River, upstream (P8) and downstream (P7) of the Garimpo areas where the rafts were seen. The *p* value indicates the statistical level of significance

compared to the dissolved fraction of the water column, as observed in the PSR data (Fig. 5b). In fact, the  $K_d$ -Hg values calculated for the RM were in the same range (2.9 to 3.8) and order of magnitude as the PSR values. Since both rivers present forests adjacent to their banks, organic matter most likely plays an important role increasing Hg affinity to the SPM (Figueiredo et al., 2011). Furthermore, reports of high Hg concentrations in the gills of detritivorous fish species in the RPS basin were attributed to the direct contact of these species with the sediment, indicating

the significant role of this compartment in Hg biota exposure (Azevedo et al., 2017), especially during the dry season (Azevedo et al., 2018). Based on the maximum Hg concentrations detected among species with different feeding habits in the region ( $0.3 \mu\text{g}\cdot\text{g}^{-1}$  wet weight; Azevedo et al., 2017) for which the safe ingestion limit established by the WHO should be exceeded ( $4 \mu\text{g}\cdot\text{kg}^{-1}$  per week per body weight; WHO, 2008), an average person (70 kg body weight) would need to eat between 1.0 and 1.5 kg of fish per week. Fish consumption in Southeastern Brazil does

not exceed 43 g per week (IBGE, 2010), so no major Hg-related health problems are expected for the population around the study areas.

*Garimpo* tailings contained higher sand contents (P9, Fig. 4c) compared to the samples from the other points, and a non-significant association between Hg concentrations and silt–clay content was observed ( $R^2=0.11$ ,  $p=0.58$ ; Fig. 4a), demonstrating a different behavior from that observed in the PSR (Fig. 4b) and at the other points of the RM (Fig. 4a). Furthermore, the tailings exhibited the highest mean Hg concentration among all environmental compartments evaluated in this study ( $197 \pm 4 \text{ ng}\cdot\text{g}^{-1}$ ), higher than the MR sediment samples ( $131 \pm 11$  and  $96 \pm 5 \text{ ng}\cdot\text{g}^{-1}$ ), in agreement with expectations. This was also observed by Odumo et al. (2014), but the Hg concentrations determined in the tailings by those authors were about 46-fold higher compared to this study. Those authors studied an area that constitutes a mining complex with a long history of this activity. Comparatively, only four rafts were identified in the sampling areas of this study, which partially explains the differences in Hg values between this study and those reported by Odumo et al. (2014).

Van Straaten (2000) reported that 20 to 30% of Hg is lost to tailings during the amalgamation process, which may explain the higher Hg concentrations observed herein. The Hg-enriched tailings on the banks of the MR can act as point sources of contamination for the ecosystem through soil leaching processes and flooding during rainy periods.

As in the PSR, the total (8 and  $10 \text{ ng}\cdot\text{L}^{-1}$ ) and dissolved Hg concentrations (4 and  $5 \text{ ng}\cdot\text{L}^{-1}$ ) in water of the MR were lower than the limits set by Brazilian regulations (2000  $\text{ng}\cdot\text{L}^{-1}$ –class III freshwater) (CONAMA, 2005). The Hg concentrations in the sediments (96 and  $131 \text{ ng}\cdot\text{g}^{-1}$ ) and in the SPM downstream the *garimpo* area ( $101 \text{ ng}\cdot\text{g}^{-1}$ , Fig. 6) were lower than those in the TEL ( $174 \text{ ng}\cdot\text{g}^{-1}$ , CCME, 2002), indicating little or no risk to the biota. However, the values observed in the SPM upstream the *garimpo* area ( $256 \text{ ng}\cdot\text{g}^{-1}$ , Fig. 6) and in the tailings ( $197 \text{ ng}\cdot\text{g}^{-1}$ ) were in the range between TEL and PEL ( $486 \text{ ng}\cdot\text{g}^{-1}$ , CCME, 2002), suggesting possible risks to the biota.

Overall, the PSR and MR had different Hg dispersion patterns. According to Moreno-Brush et al. (2020), variations in Hg concentrations in tropical river systems affected by *garimpo* activity are rarely systematic, since there is a complex network

of factors (e.g., watershed characteristics, hydrology, and specific biogeochemistry of each water body) that control the dispersion in the ecosystem. This is in line with which was observed herein. Conversely, in both rivers, Hg dynamics in the water column were mainly related to raft location, which was also reported by other studies in rivers affected by *garimpo* activity (Diringer et al., 2015; Moreno-Brush et al., 2016; Picado & Bengtsson, 2012).

## Conclusion

Illegal small-scale alluvial gold mining activities in the PSR locally impacted Hg concentrations in both fractions of the water column, sediment, and macrophytes, with limited spatial impacts. The SPM was the environmental compartment that presented the highest Hg concentration ( $95 \text{ ng}\cdot\text{g}^{-1}$ ). Sediment granulometry was essential to understand the physical impacts of *garimpo* activities on PSR silting and helped to understand the Hg dynamics in this environmental compartment, due to a high affinity to Hg. Despite the effects of *garimpo* being clear in the data, Hg concentrations in water and sediment did not exceed the limits of Brazilian and international regulations. However, it is important to emphasize that the number of mining rafts in these locations was small, so the increase in this activity can increase the environmental and health risks of the regional population. Furthermore, as only 9.38% of the entire length of the PSR was sampled, our findings are limited concerning to the impacts of *garimpo* activities throughout the entire drainage basin.

Mercury concentrations in the environmental compartments of the MR were higher than those in the PSR, which may be associated with the longer time of *garimpo* activity in this river. *Garimpo* tailings contained the highest Hg concentrations in this study and they could act as a point source of Hg contamination for the water body. Mercury concentrations in SPM and tailings from the MR have the potential to pose risks to biota. Despite a different Hg dispersion pattern in the two rivers, the SPM stands out as the main fraction of the water column in both rivers regarded Hg dynamics.

Our data demonstrate the clear effect of illegal *garimpo* activities on Hg concentrations in the environmental compartments of both rivers. It is important

to note the need for increased personnel for environmental control and monitoring and more stringent public policies aimed at the conservation of these ecosystems, since the presence of Hg poses a potential environmental risk to biota and human health. In addition, new samples should be obtained during the dry season, as the lower water column levels are expected to favor Hg remobilization. Furthermore, other Hg species should also be assessed, especially methylmercury, due to its higher bioaccumulation potential and toxicity to both wildlife and humans.

**Acknowledgements** The authors thank the Programa de Pós-Graduação em Ecologia e Recursos Naturais e Laboratório de Ciências Ambientais (LCA) of the Universidade Estadual Norte Fluminense Darcy Ribeiro (UENF) for the assistance, and the field and laboratory logistics. This work was supported by Fundação Carlos Chagas Filho de Amparo à Pesquisa do Estado do Rio de Janeiro (FAPERJ; grant numbers: E-26/111.790/2013; E-26/010.001272/2016; E-26/200.586/2022; and E-26/210.350/2022), Coordenação de Aperfeiçoamento de Pessoa de Nível Superior (CAPES, grant number: 001), and Conselho Nacional de Desenvolvimento Científico e Tecnológico (CNPq; grant number: 305.217/2017-8). UENF also supports the maintenance contract for the employed equipment. The authors also thank the anonymous reviewers for their valuable suggestions.

**Funding** Philippe R. Gomes and Inácio A. Pestana received financial support from the Coordenação de Aperfeiçoamento de Pessoal de Nível Superior (CAPES; financing code 001). Inácio A. Pestana and Carlos Eduardo de Rezende received financial support from the Fundação Carlos Chagas Filho de Amparo à Pesquisa do Estado do Rio de Janeiro (FAPERJ; grant codes E-26/200.586/2022 and E-26/010.001272/2016, respectively). Carlos Eduardo de Rezende received financial support from Conselho Nacional de Desenvolvimento Científico e Tecnológico (CNPq; grant code 305.217/2017-8).

**Data availability** The datasets generated during and/or analyzed during the current study are available from the corresponding author upon reasonable request.

**Declarations**

**Competing interests** The authors declare no competing interests.

**References**

AGEVAP. Associação pró-gestão das águas da Bacia Hidrográfica do Rio Paraíba do Sul. (2018). Relatório de situação: Bacia do Rio Paraíba do Sul. 163p. Consulted in February 2022. Available at: <https://www.ceivap.org.br/conteudo/relsituacao2018.pdf> (in Portuguese).

Alexakis, D. E. (2020). Contaminated land by wildfire effect on ultramafic soil and associated human health and ecological risk. *Land*, 9(11), 409. <https://doi.org/10.3390/land9110409>

Almeida, M. G., & Souza, C. M. M. (2008). Distribuição espacial de mercúrio total e elementar e suas interações com carbono orgânico, área superficial e distribuição granulométrica em sedimentos superficiais da bacia inferior do Rio Paraíba do Sul, RJ, Brasil. *Geochimica Brasiliensis*, 22(3), 140–158. <https://doi.org/10.21715/gb.v22i3.285> (in Portuguese).

Almeida, M. C., Cordeiro, C. E. G., Rodrigues, I. F., Moreira, M. A. C., & Villela, F. R. (2019). Destinação final de RSU no município de Campos dos Goytacazes/RJ. *Revista Mundi: Meio Ambiente e Agrárias*, 4(1), 41–56. Consulted in July 2022. Available at: <https://periodicos.ifpr.edu.br/index.php?journal=MundiMAA&page=article&op=view&path%5B%5D=41-57> (in Portuguese).

Altman, N., & Krzywinski, M. (2016). Regression diagnostics. *Nature Methods*, 13, 385–386. <https://doi.org/10.1038/nmeth.3854>

ANA. Agência Nacional de Águas. (2022). Estudos auxiliares para a gestão do risco de inundações da Bacia do rio Paraíba do Sul: Hidrografia. Consulted in February 2022. Available at: <http://gripbsul.ana.gov.br/Hidrografia.html> (in Portuguese).

ATSDR. Agency for Toxic Substances and Disease Registry. (2019). Agency for toxic substances and disease registry. Substance Priority List. Consulted in July 2022. Available at: <https://www.atsdr.cdc.gov/spl/index.html>

Azevedo, L. S., Almeida, M. G., Bastos, W. R., Suzuki, M. S., Recktenvald, M. C. N. N., Bastos, M. T. S., Vergílio, C. S., & Souza, C. M. M. (2017). Organotropismo de metilmercúrio em peixes da região sudeste do Brasil. *Chemosphere*, 185, 746–753. <https://doi.org/10.1016/j.chemosphere.2017.07.081>

Azevedo, L. S., Pestana, I. A., Rocha, A. R. M., Meneguelli-Souza, A. C., Lima, C. A. I., Almeida, M. G., Bastos, W. R., & Souza, C. M. M. (2018). Drought promotes increases in total mercury and methylmercury concentrations in fish from the lower Paraíba do Sul River, southeastern Brazil. *Chemosphere*, 202, 483–490. <https://doi.org/10.1016/j.chemosphere.2018.03.059>

Bastos, W. R., Malm, O., Pfeiffer, W. R., & Clearly, D. (1998). Establishment and analytical quality control of laboratories for Hg determination in biological and geological samples in the Amazon, Brazil. *Ciência e Cultura*, 50(4), 255–260.

Blott, S. J., Croft, D. J., Pye, K., Saye, S. E., & Wilson, H. E. (2004). Particle size analysis by laser diffraction. In: Pye, K., & Croft, D. J. (Eds.) 2004. Forensic geoscience: Principles, techniques and applications. *Geological Society, London, Special Publications*, 232, 63–73. <https://doi.org/10.1144/GSL.SP.2004.232.01.08>

Branches, D. (2021). Embarcações são destruídas em operação contra garimpo ilegal no AM. G1. Consulted in February 2022. Available at: <https://g1.globo.com/am/amazonas/noticia/2021/11/29/embarcacoes-sao-destruidas-em-operacao-contragarimpo-ilegal-no-am.html> (in Portuguese).

- Brasil. (1980). Secretaria de Defesa Sanitária Vegetal. Portaria 006 de 29 de abril. Consulted in February 2022. Available at: [https://www.camara.leg.br/proposicoesWeb/prop\\_mostrarint?eagrajssessionid=349AD13B8186C0F2AAB1ADA8BF676730.proposicoesWebExterno?codteor=1172859&filename=Dossie+-PL+3454/1980](https://www.camara.leg.br/proposicoesWeb/prop_mostrarint?eagrajssessionid=349AD13B8186C0F2AAB1ADA8BF676730.proposicoesWebExterno?codteor=1172859&filename=Dossie+-PL+3454/1980) (in Portuguese).
- Brasil. (2018). Decreto n° 9.470. Promulga a Convenção de Minamata sobre Mercúrio, firmada pela República Federativa do Brasil, em Kumamoto, em 10 de outubro de 2013. Consulted in July 2022. Available at: [https://www.in.gov.br/materia/-/asset\\_publisher/Kujrw0TZC2Mb/content/id/36849570/do1-2018-08-15-decreto-n-9-470-de-14-de-agosto-de-2018-36849564](https://www.in.gov.br/materia/-/asset_publisher/Kujrw0TZC2Mb/content/id/36849570/do1-2018-08-15-decreto-n-9-470-de-14-de-agosto-de-2018-36849564) (in Portuguese).
- Brasil. (2022a). Decreto n° 10.966. Institui o programa de apoio ao desenvolvimento da mineração artesanal e em pequena escala e a comissão interministerial para o desenvolvimento da mineração artesanal e em pequena escala (Pró-Mape). Consulted in February 2022. Available at: <https://www.in.gov.br/en/web/dou/-/decreto-n-10.966-de-11-de-fevereiro-de-2022-379739340> (in Portuguese).
- Brasil. (2022b). Decreto n° 10.965. Simplifica processos e outorgas de títulos minerários. Consulted in February 2022. Available at: <https://www.in.gov.br/en/web/dou/-/decreto-n-10.965-de-11-de-fevereiro-de-2022-379739232> (in Portuguese).
- Câmara, V. M. (1986). Estudo comparativo dos efeitos tardios dos fungicidas organo-mercuriais no município de Campos – RJ. Tese, ENSP/FIOCRUZ, Rio de Janeiro, Brasil. 283p (in Portuguese).
- Câmara, V. M. (1990). O caso de Campos-RJ: Estudo do quadro de morbidade causado pela exposição progressiva dos trabalhadores após fungicidas organo-mercuriais. In S. Hacon, L. D. Lacerda, W. C. Pfeiffer, & D. Carvalho (Eds.), *Riscos e consequências do Uso do Mercúrio* (pp. 229–246p). FINEP/CNPq/MS/IBAMA (in Portuguese).
- Câmara, V. M. (2017). Contributions to the epidemiological study design on mercury pollution in Amazon. *Revista Pan-Amazônica De Saúde*, 8(4), 1–4. <https://doi.org/10.5123/s2176-62232017000400004>
- CCME. Canadian Council of Ministers of the Environment. (2002). Canadian sediment quality guidelines for the protection of aquatic life - Protocol for the derivation of Canadian sediment quality guidelines for the protection of aquatic life. Consulted in February 2022. Available at: <https://ccme.ca/en/res/protocol-for-the-derivation-of-canadian-sediment-quality-guidelines-for-the-protection-of-aquatic-life-en.pdf>
- Cheng, H., & Hu, Y. (2012). Mercury in municipal solid waste in China and its control: A review. *Environmental Science & Technology*, 16(2), 593–605. <https://doi.org/10.1021/es2026517>
- CONAMA. Conselho Nacional do Meio Ambiente. (2005). Resolução n° 357. Dispõe sobre a classificação dos corpos de água e diretrizes ambientais para o seu enquadramento, bem como estabelece as condições e padrões de lançamento de efluentes, e dá outras providências. Consulted in February 2022. Available at: [https://icmbio.gov.br/cepsul/images/stories/legislacao/Resolucao/2005/res\\_conama\\_357\\_2005\\_classificacao\\_corpos\\_agua\\_rtfcd\\_a\\_ltrd\\_res\\_393\\_2007\\_397\\_2008\\_410\\_2009\\_430\\_2011.pdf](https://icmbio.gov.br/cepsul/images/stories/legislacao/Resolucao/2005/res_conama_357_2005_classificacao_corpos_agua_rtfcd_a_ltrd_res_393_2007_397_2008_410_2009_430_2011.pdf) (in Portuguese).
- Dall'Agnol, R., Sahoo, P. K., Salomão, G. N., de Araújo, A. D. M., da Silva, M. S., Powell, M. A., Junior, J. F., Ramos, S. J., Martins, G. C., da Costa, M. F., & Guilherme, L. R. G. (2022). Soil-sediment linkage and trace element contamination in forested/deforested areas of the Itacaiúnas River Watershed, Brazil: To what extent land-use change plays a role? *Science of the Total Environment*, 828, 154327. <https://doi.org/10.1016/j.scitotenv.2022.154327>
- Diringer, S. E., Feingold, B. J., Ortiz, E. J., Gallis, J. A., Araújo-Flores, J. M., Berky, A., Pan, W. K. Y., & Hsu-Kim, H. (2015). River transport of mercury from artisanal and small-scale gold mining and risks for dietary mercury exposure in Madre de Dios, Peru. *Environmental Science: Processes & Impacts*, 17(2), 478–487. <https://doi.org/10.1039/c4em00567h>
- DNPM. Departamento Nacional de Produção Mineral. (1983). Projeto RADAMBRASIL, Levantamento de Recurso Naturais 32, Folhas SF.23/24. Ministério de Minas e Energia, 780p. (in Portuguese).
- Esdaile, L. J., & Chalker, J. M. (2018). The mercury problem in artisanal and small-scale gold mining. *Chemistry—a European Journal*, 24(27), 6905–6916. <https://doi.org/10.1002/chem.201704840>
- Figueiredo, R. O., Ovalle, A. R., Rezende, C. E., & Martinelli, L. A. (2011). Carbon and nitrogen in the lower basin of the Paraíba do Sul River, Southeastern Brazil: Element fluxes and biogeochemical processes. *Revista Ambiente & Água*, 6(2), 7–37. <https://doi.org/10.4136/ambi-agua.183>
- Folha de Itálva. (2021a). PF realiza operação Paraíba Dourado contra extração de ouro em Cambuci e São Fidélis. Consulted in February 2022. Available at: <https://folhadeitalva.com.br/2021/11/11/pf-realiza-operacao-paraiba-dourado-contra-extracao-de-ouro-em-cambuci-e-sao-fidelis/> (in Portuguese).
- Folha de Itálva. (2021b). Uenf investiga presença de mercúrio em amostras do Rio Muriaé nas proximidades de Itálva. Consulted in February 2022. Available at: <https://folhadeitalva.com.br/2021/12/07/uenf-investiga-presenca-de-mercúrio-em-amostras-do-rio-e-muriaenas-proximidades-de-italva/> (in Portuguese).
- Franz, C., Makeschin, F., Weiß, H., & Lorz, C. (2013). Geochemical signature and properties of sediment sources and alluvial sediments within the Lago Paranoá catchment, Brasília DF: A study on anthropogenic introduced chemical elements in an urban river basin. *Science of the Total Environment*, 452, 411–420. <https://doi.org/10.1016/j.scitotenv.2013.02.077>
- Gamvroula, D., Alexakis, D., & Stamatis, G. (2013). Diagnosis of groundwater quality and assessment of contamination sources in the Megara basin (Attica, Greece). *Arabian Journal of Geosciences*, 6(7), 2367–2381. <https://doi.org/10.1007/s12517-012-0533-6>
- Guimaraes, J. R. (2020). Mercury in the Amazon: Problem or opportunity? A commentary on 30 years of research on the subject. *Elementa: Science of the Anthropocene*. <https://doi.org/10.1525/elementa.032>
- Hacon, S., Lacerda, L. D., Pfeiffer, W., & Carvalho, D. (1990). Riscos e consequências do uso do mercúrio. Rio de Janeiro. FINEP, Rio de Janeiro, p. 314 (in Portuguese).
- IBGE. Instituto Brasileiro de Geografia e Estatística. (2010). Aquisição alimentar domiciliar per capita anual por grupos, subgrupos e produtos. Pesquisa de Orçamentos

- Familiares em 2008–2009. Consulted in July 2022. Available at: <https://sidra.ibge.gov.br/home/pms/brasil> (in Portuguese).
- IBGE. Instituto Brasileiro de Geografia e Estatística. (2021). Cidades e Estados: Campos dos Goytacazes. Consulted in July 2022. Available at: <https://www.ibge.gov.br/cidades-e-estados/rj/campos-dos-goytacazes.html> (in Portuguese).
- Jornal Terceira Via. (2021). Uenf investiga presença de mercúrio em amostras dos Rios Paraíba do Sul e Muriaé. Consulted in February 2022. Available at: <https://www.jornalterceiravia.com.br/2021/12/06/uenf-investiga-presenca-de-mercúrio-em-amostras-dos-rios-paraiba-do-sul-e-muriae/> (in Portuguese).
- Kasper, D., Forsberg, B. R., Almeida, R., Bastos, W. R., & Malm, O. (2015). Methodologies for sampling, preservation and storage of water samples for mercury analysis – A review. *Química Nova*, 38(3), 410–418. <https://doi.org/10.5935/0100-4042.20150020>
- Khitalishvili, K. (2016). Monte Carlo simulation in R: basic example. Consulted in February 2022. Available at: <https://rpubs.com/Koba/Monte-Carlo-Basic-Example>
- Krumbein, W. C., & Aberdeen, E. (1937). The sediments of Barataria bay. *Journal of Sedimentary Petrology*, 7(1), 3–17. <https://doi.org/10.1306/D4268F8B-2B26-11D7-8648000102C1865D>
- Lacerda, L. D., & Ribeiro, M. G. (2004). Changes in lead and mercury atmospheric deposition due to industrial emissions in Southeastern Brazil. *Journal of the Brazilian Chemical Society*, 15(6), 931–937. <https://doi.org/10.1590/S0103-50532004000600022>
- Lacerda, L. D., & Malm, O. (2008). Mercury contamination in aquatic ecosystems: An analysis of the critical areas. *Estudos Avançados*, 22(63), 173–190. <https://doi.org/10.1590/S0103-40142008000200011>
- Lacerda, L. D., Carvalho, C. E. V., Rezende, C. E., & Pfeiffer, W. C. (1993). Mercury in sediments from the Paraíba do Sul River Continental Shelf, S.E., Brazil. *Marine Pollution Bulletin*, 26(4), 220–222. [https://doi.org/10.1016/0025-326X\(93\)90626U](https://doi.org/10.1016/0025-326X(93)90626U)
- Lauthartte, L. C., Gomes, D. F., Mussu, M. H., Holanda, I. B. B., Almeida, R., & Bastos, W. R. (2018). Potencial exposição ao mercúrio atmosférico no ambiente ocupacional de comércio de ouro de Porto Velho, Rondônia. *Química Nova*, 41(9), 1055–1060. <https://doi.org/10.21577/0100-4042.20170253> (in Portuguese).
- Lechler, P. J., Miller, J. R., Lacerda, L. D., Vinson, D., Bonzongo, J. C., Lyons, W. B., & Warwick, J. J. (2000). Elevated mercury concentrations in soils, sediments, water, and fish of the Madeira River basin, Brazilian Amazon: A function of natural enrichments? *Science of the Total Environment*, 260(1), 87–96. [https://doi.org/10.1016/S0048-9697\(00\)00543-X](https://doi.org/10.1016/S0048-9697(00)00543-X)
- Li, P., Yang, Y., & Xiong, W. (2015). Impacts of mercury pollution controls on atmospheric mercury concentration and occupational mercury exposure in a hospital. *Biological Trace Element Research*, 168(2), 330–334. <https://doi.org/10.1007/s12011-015-0391-7>
- Lima, E. C. R. (1990). Riscos e conseqüências do uso de mercúrio: a situação do Rio de Janeiro In: Riscos e conseqüências do uso de mercúrio. Finep/CNPQ/MS/IBAMA, Rio de Janeiro, pp. 268–274 (in Portuguese).
- Limbong, D., Kumampung, J., Rimper, J., Arai, T., & Miyazaki, N. (2003). Emissions and environmental implications of mercury from artisanal gold mining in north Sulawesi, Indonesia. *Science of the Total Environment*, 302(1–3), 227–236. [https://doi.org/10.1016/S0048-9697\(02\)00397-2](https://doi.org/10.1016/S0048-9697(02)00397-2)
- Lominchar, M. A., Sierra, M. J., Jiménez-Moreno, M., Guirado, M., Rodríguez, R. C. D. M., & Millán, R. (2019). Mercury species accumulation and distribution in *Typha domingensis* under real field conditions (Almaden, Spain). *Environmental Science and Pollution Research*, 26(4), 3138–3144. <https://doi.org/10.1007/s11356-018-1861-1>
- McCave, I. N., Bryant, R. J., Cook, H. F., & Coughanowr, C. A. (1986). Evaluation of a laser-diffraction-size analyzer for use with natural sediments: Research method paper. *Journal of Sedimentary Petrology*, 56(4), 561–564.
- Mendiburu, F. (2021). Agricolae: Statistical procedures for agricultural research. R package version 1.3–5. Consulted in February 2022. Available at: <https://CRAN.R-project.org/package=agricolae>
- Meneses, H. N. M., Oliveira-da-Costa, M., Basta, P. C., Morais, C. G., Pereira, R. J. B., Souza, S. M. S., & Hacon, S. S. (2022). Mercury contamination: A growing threat to riverine and urban communities in the Brazilian Amazon. *International Journal of Environmental Research and Public Health*, 19(5), 2816. <https://doi.org/10.3390/ijerph19052816>
- Mol, J. H., & Ouboter, P. E. (2004). Downstream effects of erosion from small-scale gold mining on the instream habitat and fish community of a small neotropical rainforest stream. *Conservation Biology*, 18(1), 201–214. Consulted in February 2022. Available at: <http://www.jstor.org/stable/3589131>
- Molisani, M. M., Rocha, R., Machado, W., Barreto, R. C., & Lacerda, L. D. (2006). Mercury contents in aquatic macrophytes from two reservoirs in the Paraíba do Sul: Guandú river system, SE Brazil. *Brazilian Journal of Biology*, 66(1A), 101–107. <https://doi.org/10.1590/S1519-69842006000100013>
- Moreno-Brush, M., McLagan, D. S., & Biester, H. (2020). Fate of mercury from artisanal and small-scale gold mining in tropical rivers: Hydrological and biogeochemical controls. A critical review. *Critical Reviews in Environmental Science and Technology*, 50(5), 437–475. <https://doi.org/10.1080/10643389.2019.1629793>
- Moreno-Brush, M., Rydberg, J., Gamboa, N., Storch, I., & Biester, H. (2016). Is mercury from small-scale gold mining prevalent in the southeastern Peruvian Amazon? *Environmental Pollution*, 218, 150–159. <https://doi.org/10.1016/j.envpol.2016.08.038>
- Odumo, B. O., Carbonell, G., Angeyo, H. K., Patel, J. P., Torrijos, M., & Martín, J. A. R. (2014). Impact of gold mining associated with mercury contamination in soil, biota sediments and tailings in Kenya. *Environmental Science and Pollution Research*, 21(21), 12426–12435. <https://doi.org/10.1007/s11356-014-3190-3>
- Passos, C. J., & Mergler, D. (2008). Human mercury exposure and adverse health effects in the Amazon: A review. *Cadernos De Saúde Pública*, 24(S4), 503–520. <https://doi.org/10.1590/S0102-311X2008001600004>
- Pestana, I. A., Almeida, M. G., Bastos, W. R., & Souza, C. M. M. (2019). Total Hg and methylmercury dynamics in a

- river-floodplain system in the Western Amazon: Influence of seasonality, organic matter and physical and chemical parameters. *Science of the Total Environment*, 656(1), 388–399. <https://doi.org/10.1016/j.scitotenv.2018.11.388>
- Pestana, I. A., Rezende, C. E., Almeida, R., Lacerda, L. D., & Bastos, W. R. (2022). Let's talk about mercury contamination in the Amazon (again): The case of the floating gold miners' village on the Madeira River. *The Extractive Industries and Society*. <https://doi.org/10.1016/j.exis.2022.101122>
- Pfeiffer, W. C., & Lacerda, L. D. (1988). Mercury inputs into the Amazon Region, Brazil. *Environmental Technology Letters*, 9(4), 325–330. <https://doi.org/10.1080/09593338809384573>
- Picado, F., & Bengtsson, G. (2012). Temporal and spatial distribution of waterborne mercury in a gold miner's river. *Journal of Environmental Monitoring*, 14(10), 2746–2754. <https://doi.org/10.1039/C2EM30203A>
- Pontes, F. (2021). Ribeirinhos convertem-se ao ouro e desafiam contaminação por mercúrio no rio Madeira. (o)eco. Consulted in July 2022. Available at: <https://oeco.org.br/reportagens/ribeirinhos-convertem-se-ao-ouro-e-desafiam-contaminacao-por-mercúrio-no-rio-madeira/> (in Portuguese).
- Prazeres, L. P. (2021). Garimpo na Amazônia: o que está por trás da invasão do rio Madeira. BBC NEWS Brasil, 2021. Consulted in February 2022. Available at: <https://www.bbc.com/portuguese/brasil-59425015> (in Portuguese).
- R Core Team. (2021). R: A language and environment for statistical computing. R Foundation for Statistical Computing. Austria, Vienna. Consulted in February 2022. Available at: <http://www.R-project.org/>
- Rocha, A. R. M., Di Benedito, A. P. M., Pestana, I. A., & Souza, C. M. M. (2015). Isotopic profile and mercury concentration in fish of the lower portion of the rio Paraíba do Sul watershed, southeastern Brazil. *Neotropical Ichthyology*, 13(4), 723–732. <https://doi.org/10.1590/1982-0224-20150047>
- Sarwar, N., Imran, M., Shaheen, M. R., Ishaque, W., Kamran, M. A., Matloob, A., Rehim, A., & Hussain, S. (2017). Phytoremediation strategies for soils contaminated with heavy metals: Modifications and future perspectives. *Chemosphere*, 171, 710–721. <https://doi.org/10.1016/j.chemosphere.2016.12.116>
- Selin, N. E. (2009). Global biogeochemical cycling of mercury: A review. *Annual Review of Environment and Resources*, 34(1), 43–63. <https://doi.org/10.1146/annurev.environ.051308.084314>
- Serapião, F., & Ladeira, P. (2022). Garimpo e desmatamento sujam água em Alter do Chão, conclui laudo; veja vídeo. Consulted in July 2022. Available at: <https://www1.folha.uol.com.br/ambiente/2022/02/garimpo-e-desmatamento-sujaram-agua-em-alter-do-chao-conclui-laudo.shtml> (in Portuguese).
- Silva-Filho, E. V., Machado, W., Oliveira, R. R., Sella, S. M., & Lacerda, L. D. (2006). Mercury deposition through litterfall in an Atlantic Forest at Ilha Grande, Southeast Brazil. *Chemosphere*, 65, 2477–2484. <https://doi.org/10.1016/j.chemosphere.2006.04.053>
- Souza, C. M. M. (1994). Avaliação ambiental dos riscos do mercúrio em áreas de garimpo de Brasil. PhD Thesis, Universidade Federal do Rio de Janeiro, Rio de Janeiro, Brasil (in Portuguese).
- Suárez, Y. R., Petrere, M., Jr., & Catella, A. C. (2001). Factors determining the structure of fish communities in Pantanal lagoons (MS, Brazil). *Fisheries Management and Ecology*, 8(2), 173–186. <https://doi.org/10.1046/j.1365-2400.2001.00236.x>
- Thomas, J. A. (2021). Países importadores de ouro do Brasil estimulam garimpo ilegal na Amazônia. MONGABAY, 2021. Consulted in February 2022. Available at: <https://brasil.mongabay.com/2021/10/paises-importadores-de-ouro-do-brasil-estimulam-garimpo-ilegal-na-amazonia/> (in Portuguese).
- Trindade, O. (2021). Extração ilegal de ouro no Rio Paraíba do Sul chama a atenção. Jornal Terceira Via. Consulted in February 2022. Available at: <https://www.jornalterceiravia.com.br/2021/11/28/extracao-ilegal-de-ouro-no-rio-paraiba-do-sul-chama-atencao/> (in Portuguese).
- UNEP. United Nations Environment Programme. (2013). United nations environment programme. Minamata convention agreed by nations. Consulted in July 2022. Available at: <https://www.unep.org/news-and-stories/press-release/minamata-convention-agreed-nations>
- UNEP. United Nations Environment Programme. (2017). World Unites Against Mercury Pollution. Consulted in July 2022. Available at: <https://unep.org/news-and-stories/press-release/world-unites-against-mercury-pollution>
- UNEP. United Nations Environment Programme. (2019). Global Mercury Assessment 2018. Chemicals and Health Branch Geneva, Switzerland. 62 pp. ISBN: 978-92-807-3744-8. Consulted in July 2022. Available at: <https://wedocs.unep.org/bitstream/handle/20.500.11822/27579/GMA2018.pdf>
- van Straaten, P. (2000). Mercury contamination associated with small-scale gold mining in Tanzania and Zimbabwe. *Science of the Total Environment*, 259(1–3), 105–113. [https://doi.org/10.1016/S0048-9697\(00\)00553-2](https://doi.org/10.1016/S0048-9697(00)00553-2)
- Veeck, L., Silva-Filho, E. V., Wasserman, J. C., Sella, S. M., Santos, I. R., & Lacerda, L. D. (2007). Mercury distribution in sediments of a sub-tropical coastal lagoon, Sepetiba Bay, SE Brazil. *Geochimica Brasiliensis*, 21(1), 50–57. Consulted in July 2022. Available at: <https://geobrasiliensis.emnuvens.com.br/geobrasiliensis/article/view/256>
- Venables, W. N., & Ripley, B. D. (2002). Modern applied statistics with S. Fourth Edition. Springer, New York. ISBN 0-387-95457-0.
- WHO. World Health Organization. (2008). Guidance for identifying populations at risk from mercury exposure. Inter-Organization Programme for the Sound Management of Chemicals. Consulted in July 2022. Available at: <https://wedocs.unep.org/20.500.11822/11786>

**Publisher's Note** Springer Nature remains neutral with regard to jurisdictional claims in published maps and institutional affiliations.

Springer Nature or its licensor holds exclusive rights to this article under a publishing agreement with the author(s) or other rightsholder(s); author self-archiving of the accepted manuscript version of this article is solely governed by the terms of such publishing agreement and applicable law.